

Bipolar anthracene derivatives containing hole- and electron-transporting moieties for highly efficient blue electroluminescence devices†

Jinhai Huang,^a Jian-Hua Su,^a Xin Li,^a Mei-Ki Lam,^b Ka-Man Fung,^b Hai-Hua Fan,^b Kok-Wai Cheah,^b Chin H. Chen^{bc} and He Tian^{*a}

Received 1st October 2010, Accepted 22nd November 2010

DOI: 10.1039/c0jm03300f

A series of bipolar anthracene derivatives containing hole-transporting triphenylamine and electron-transporting benzimidazole moieties were synthesized and characterized. These compounds possess high thermal properties and quantum yield in toluene solution but their photoluminescence spectra are sensitive to the polarity of the solvent. Three types of devices were fabricated to investigate their electron-transporting and hole-transporting as well as light-emitting properties. The electroluminescence spectra for the three derivatives B1, B3 and B4 show that they emit blue light, while the B2-based devices produced white light at a low current density because of the electromer formation. Moreover, a single layer OLED device for B4 exhibited a current efficiency of 3.33 cd A⁻¹ with a pure blue color of CIE_(x,y) of (0.16, 0.16) at 20 mA cm⁻² and a maximum brightness of 8472 cd m⁻² at 8.7 V.

Introduction

Organic light-emitting diodes (OLEDs) have drawn great scientific and commercial attention, due to their potential applications in full-color, flat-displays as well as solid-state lighting.^{1–3} A typical trilayer electroluminescent (EL) device consists of a light-emitting layer, an electron-transporting layer, as well as a hole-transporting layer. Therefore, the EL performance significantly depends on the recombination efficiency of the holes and electrons injected from the anode and cathode, respectively.⁴ Large efforts are devoted to optimizing the charge flux balance for improving the device efficiency and limiting the energy consumption, because the hole-transporting material has a higher carrier drift than the electron-transporting material in most OLEDs materials.^{5,6}

Bipolar materials with emission characteristics incorporating both hole- and electron-transporting segments can effectively stabilize exciton formation and balance the hole and electron charge in the emitting layer.⁷ Moreover, the utilization of bipolar compounds will significantly simplify the device structure with double layers or even a single layer, which will largely limit the

overall cost and accelerate its ongoing commercialization activities. Considerable progress has been reported to apply the bipolar molecules in the OLEDs.^{8–15} However, the donor–acceptor system will bring out some serious disadvantages of the bipolar materials in OLEDs, such as a huge bathochromic effect,¹⁶ low quantum yield due to the dipolar quenching,¹⁷ easy crystallization due to large dipolar moment,¹⁷ as well as the low band gap of the materials owing to the intermolecular charge transfer.¹⁸ Hence, compared to the efficient and stable red and green device, sufficiently wide band gap of highly efficient and stable bipolar blue luminescent materials are still rare.^{19,20} In addition, blue emission materials play a particularly important role in the development of OLEDs, which can not only be used as a blue light source in their own right,²¹ but also can be utilized to generate light of green and red color by energy cascade to a suitable emissive dopant.²²

Anthracene has been intensively studied as an attractive building block and starting material in OLEDs, due to its unusual photoluminescence and electroluminescence properties and excellent electrochemical properties, as well as easier modification. The anthracene derivatives imply multifunctional properties through introducing different groups, such as light-emitting layer,²³ hole-transporting layer,^{23f,24} and electron-transporting layer.^{23e,25} As the light-emitting layer, the fluorescence spectra color of anthracene derivatives can be easily tuned from blue to green by importing different bulks at the C-9 and 10 positions.²³ Moreover, the white OLEDs based on the anthracene derivatives were also achieved in a single component system.²⁶

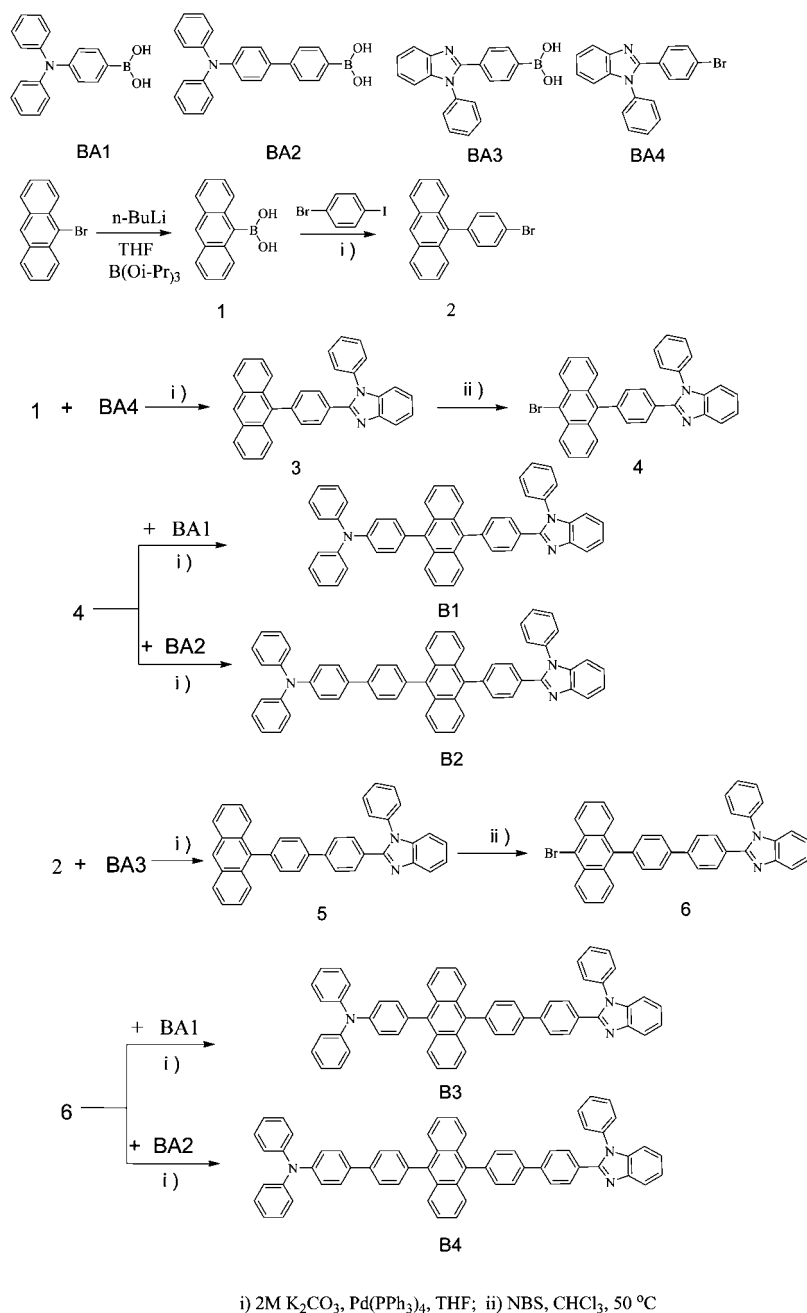
In this paper, we synthesized a series of bipolar blue lighting materials containing a hole-transporting triphenylamine moiety and an electron-transporting benzimidazole moiety at the C-9

^aKey Laboratory for Advanced Materials and Institute of Fine Chemicals, East China University of Science & Technology, Shanghai, 200237, China. E-mail: tianhe@ecust.edu.cn; Fax: (+86) 21-64252288

^bCentre for Advanced Luminescence Materials, Department of Physics, Hong Kong Baptist University, Kowloon Tong, Hong Kong, China

^cDisplays & Lighting Center, National Engineering Lab of TFT-LCD Materials and Technologies, Shanghai Jiao Tong University, Shanghai, 200240, China

† Electronic supplementary information (ESI) available: The absorption spectra and fluorescence spectra of B2 and B3, the TGA and DSC curves of target compounds, the device performance of B1 and B2, and the EL spectra of device I–III for B2. See DOI: 10.1039/c0jm03300f



Scheme 1 The synthetic routes of the bipolar compounds.

and C-10 positions of the anthracene. The color and the energy levels were modified by the phenyl bridge between the functionalized moieties and the anthracene core. The thermal properties and photophysical properties were fully investigated. The HOMO and LUMO values were measured by cyclic voltammetry. In addition, a series of devices were fabricated to systematically study the hole-transporting and electron-transporting and the emitting properties of these bipolar anthracene derivatives. We achieved a current efficiency of 3.33 cd A⁻¹ with a pure blue CIE_(x,y) of (0.16, 0.16) at 20 mA cm⁻² and a maximum brightness of 8472 cd m⁻² at 8.7 V in a single layer device for B4, which has one of the best pure blue electroluminescence performances among the reported single-layer devices.^{8–20}

Results and discussions

Synthesis

The synthetic routes to the bipolar compounds are illustrated in Scheme 1. Some starting materials were synthesized according to the literatures in good yield. The 9-anthracene boronic acid was obtained by reacting 9-bromoanthracene and *n*-BuLi and triisopropylborate in good yield. Suzuki aryl-aryl coupling reactions and bromination reactions were employed in the synthesis of the intermediates with a yield of over 70%. The target compounds were also achieved by the boronate compounds reacting with bromides through Suzuki aryl-aryl coupling reactions. The compounds were available purified with the silica

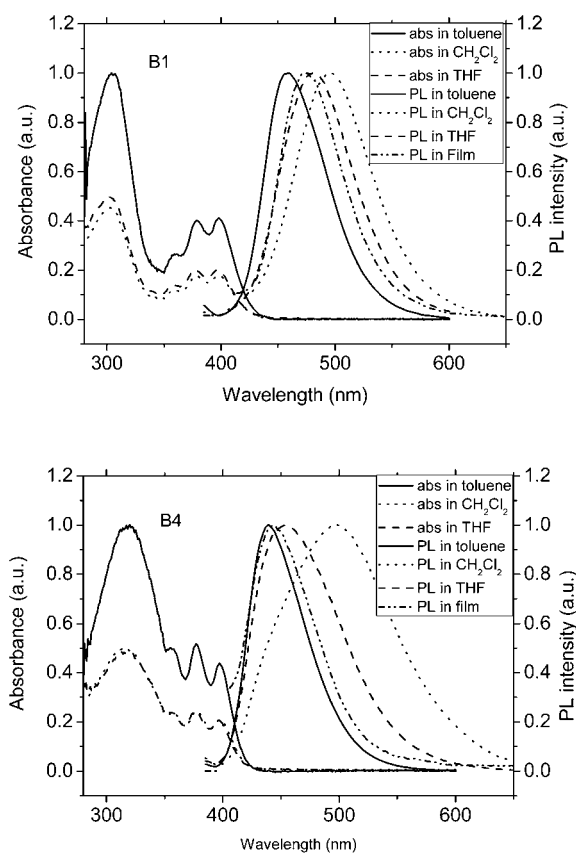


Fig. 1 The absorption spectra and fluorescence spectra (excited at 380 nm) of B1 and B4.

column chromatographic method or recrystallization in the common solvents except the B4, which can be obtained by simple filtration from the reaction mixture, because of whose poor solubility. The compounds were verified by ^1H NMR, ^{13}C NMR and high-resolution mass spectrometry. Compound B4 was confirmed by MALDI-TOF-MS spectrum with only one peak at 842.3582.

Photophysical properties

The UV-vis and PL spectra of the bipolar anthracene derivatives in three different solvents (toluene, THF, and dichloromethane) as well as in the solid thin film spin-coated with PMMA on quartz plates were measured as shown in Fig. 1 and Fig. S1.† A summary of the photophysical data of these compounds is also given in Table 1. There is no obvious solvatochromism in the absorption spectra. These four compounds exhibit the rather

similar absorption bands in the range of 350–400 nm, which were assigned to the π - π^* transition of the characteristic vibrational structures of the isolated anthracene groups. Moreover, the absorption was not affected by the phenyl bridge length, this was due to the lack coplanarity of biphenyl group and a twisting angle of about 60° caused by the steric interactions of 9,10-phenyl rings with hydrogen atoms in the peri-positions of the anthracene unit.^{21,27}

Because the twist between the anthracene and phenyl rings can effectively reduce the charge transfer from the triphenylamine moiety to the benzimidazole moiety, these compounds emit light in the blue region. In comparison with the absorption spectra, the emission spectra are sensitive to the polarity of the solvent (see Fig. 1 and S1†). Especially, pronouncedly red-shifted and broadened spectra were found in CH_2Cl_2 for all the compounds. This phenomenon can be explained by the solvent stabilization of the excited state and dipolar interactions between the bipolar compounds and the polar solvents.²⁸ The emission spectra in the film for all the materials are located between that for toluene and THF solutions in the blue region, implying that no significant intermolecular interactions occur in the ground state. These derivatives indicate a high quantum yield in toluene because of the presence of the anthracene moiety. It is noteworthy that quantum yield increase with the increase of the phenyl rings, because less coplanarity and less π -electron conjugation of phenyl ring could reduce energy wastage in charge transfer and even nonradiative decay.

Thermal properties

The thermal properties of these compounds were determined by thermogravimetric analysis (TGA) and differential scanning calorimetry (DSC). The key data were listed in Table 2. TGA, with a heat rate of $20^\circ\text{C min}^{-1}$ under N_2 , indicates the decomposition temperatures (T_d ; corresponding to 5% weight loss) for B1, B2, B3, and B4 with as high as 460.4°C , 481.0°C , 486.0°C , and 519.7°C , respectively, increasing as the phenyl rings increase (see Fig. S2†). The melting points of B1, B2, and B4 (310.6°C , 349.8°C and 398.8°C , respectively) are higher than that for B3 (276.1°C), detected by the DSC, since the molecular symmetry and weight are effectively beneficial to the melting point. The T_g values for B1, B2 and B3 are 144.1°C , 152.7°C , and 161.5°C , respectively. The T_g of B4 was not found in the DSC curves. Fig. S3 showed the repeated DSC heating scan for T_g of B1.† The high thermal properties of these compounds are of importance to retain stable film morphological properties during the device operation, which are also desirable for good performance of OLEDs with high stability and efficiency.

Table 1 The photophysical data for B1–4

	λ_{abs} (nm)			λ_{em} (fwhm)(nm) ^a				Φ_f^b
	Toluene	CH_2Cl_2	THF	Toluene	CH_2Cl_2	THF	Film	
B1	304, 359, 379, 398	303, 360, 378, 398	303, 359, 378, 397	459 (63)	496 (80)	481 (75)	475 (65)	0.55
B2	309, 358, 377, 398	306, 357, 377, 397	306, 356, 376, 396	440 (56)	496 (84)	461 (93)	452 (69)	0.73
B3	308, 357, 378, 398	309, 357, 378, 397	309, 357, 378, 396	457 (62)	493 (79)	477 (73)	472 (66)	0.60
B4	320, 357, 377, 397	315, 357, 377, 397	315, 357, 377, 397	439 (57)	498 (118)	454 (86)	444 (68)	0.82

^a Excited at 380 nm. ^b PL quantum yield relative to 9,10-diphenylanthracene(DPA) in cyclohexane ($\Phi_f = 0.90$).

Table 2 The physical data for B1–4

	T_g (°C) ^a	T_m (°C) ^a	T_d (°C) ^b	HOMO (eV) ^c	LUMO (eV) ^c	E_g (eV) ^d	HOMO (eV) ^e	LUMO (eV) ^e	E_g (eV) ^e
B1	144.1	310.6	460.4	5.33	2.40	2.93	4.97	1.62	3.35
B2	152.7	349.8	481.0	5.29	2.32	2.97	4.95	1.64	3.31
B3	161.5	276.1	486.0	5.33	2.41	2.92	4.97	1.63	3.34
B4	not available	398.8	519.7	5.28	2.32	2.96	4.95	1.62	3.33

^a Determined by DSC measurement with a heating and cooling rate of 20 °C min⁻¹ under N₂. ^b Determined by TGA with a heating rate of 20 °C min⁻¹ under N₂. ^c Obtained by CV in CH₂Cl₂. All the potentials were calculated relative to ferrocene. LUMO energy was estimated based on the HOMO levels and E_g . ^d Determined from the absorption threshold. ^e Theoretical calculations with B3LYP/6-31G.

Electrochemical properties

The electrochemical properties of the bipolar compounds, studied by the cyclic voltammetry (CV) analyses in CH₂Cl₂ solution, are revealed in Table 2. The HOMO levels for B1–B4 are around 5.3 eV, which are higher than that for other anthracene derivatives, due to the electron-donating triphenylamine moiety. The higher HOMO values are close to the work function of ITO, which can effectively decrease the energy barrier of hole injection and improve the device efficiency. The CV curves of these materials with a quasi-reversible two-electron oxidation are attributable to the triphenylamine and anthracene group. The wide optical energy band gaps (E_g) were found about 2.95 eV, determined from the threshold of UV-vis absorption spectra, and then used to calculate the LUMO levels. The electrochemical properties of these four compounds are almost identical, which are in agreement with the behavior of the photophysical properties.

Theoretical calculations

The three-dimensional geometries and the frontier molecular orbital energy levels of these bipolar anthracene derivatives were calculated using density functional theory (DFT). The calculations of the HOMO and LUMO levels were depicted in Table 2. The theoretical values of the HOMO and LUMO levels for the four compounds are almost identical. Fig. 2 shows the calculated optimized geometries and spatial distributions of the compounds B1–4. The presence of large dihedral angles (about 79–88° between the anthracene and the phenyl rings and about 36° between the biphenyl linkage according to the theoretical calculations) will be useful to keep the unique properties of each functional segments and decrease their interaction. As shown in Fig. 2, the electron densities of HOMO for B1 and B3 are mostly localized on the triphenylamine and anthracene units, while those for B2 and B4 are mainly populated over the triphenylamine moieties. Compared to the separation of spacial distributions of B2 and B4 between the triphenylamine and anthracene, those of B1 and B3 partially encompass the central anthracene, which will promote B1 and B3 to emit longer wavelength light than B2 and B4. Moreover, based on the especial electron densities, we can easily explain why the HOMO level of B1 and B3 is about 0.04 eV lower than that of B2 and B4. However, the LUMOs for all compounds are localized on the anthracene units. The spacial distribution of HOMO and LUMO is desirable to improve the charge transport.

Electroluminescent properties

To investigate the hole-transporting properties, electron-transporting properties, and light-emitting properties, we fabricated three types of devices, with the device configurations: **device I**: ITO/NPB (40 nm)/B1–4 (40 nm)/LiF (1 nm)/Al (100 nm); **device II**: ITO/B1–4 (40 nm)/TPBI (40 nm)/LiF (1 nm)/Al (100 nm); and **device III**: ITO/NPB (40 nm)/B1–4 (40 nm)/TPBI (20 nm)/LiF (1 nm)/Al (100 nm). 4,4'-bis[*N*-(1-naphthyl)-*N*-phenyl-1-amino]-biphenyl (NPB) was used as the hole-transporting layer, TPBI was used as the electron-transporting layer, and LiF and Al were used as the electron injecting layer and cathode, respectively.

The device performances for the bipolar compounds were listed in Table 3 and Table S1.† The current density-voltage-luminance (I - V - L) and current density-current efficiency characteristics for the compound B4 were shown in Fig. 3 and Fig. 4. Compared to other compounds, the compound B1 showed the lowest device performance. For example, the current efficiency of the device III at a current density of 20 mA cm⁻² for B2, B3, and

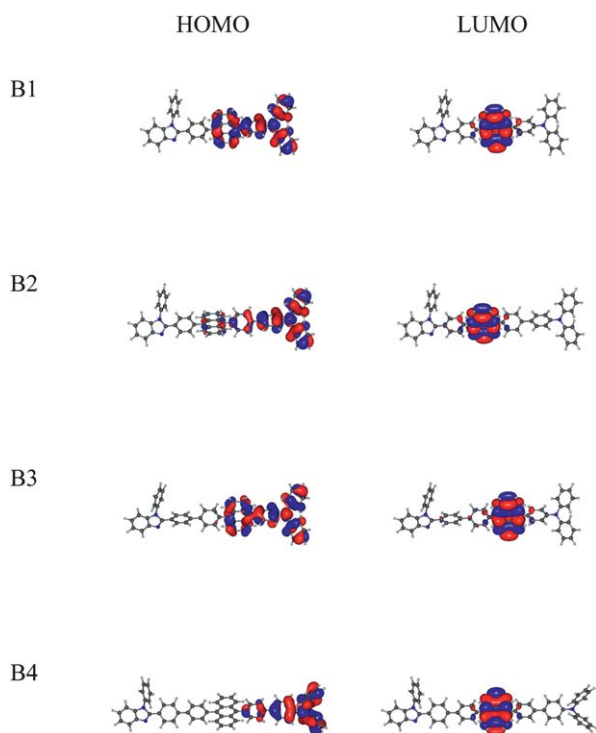


Fig. 2 Calculated optimized geometries and spatial distributions of B1–4.

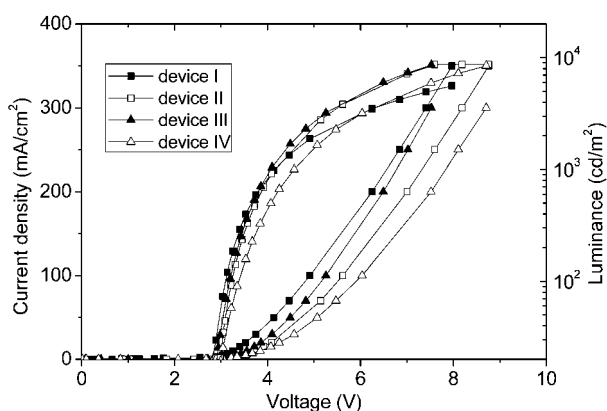
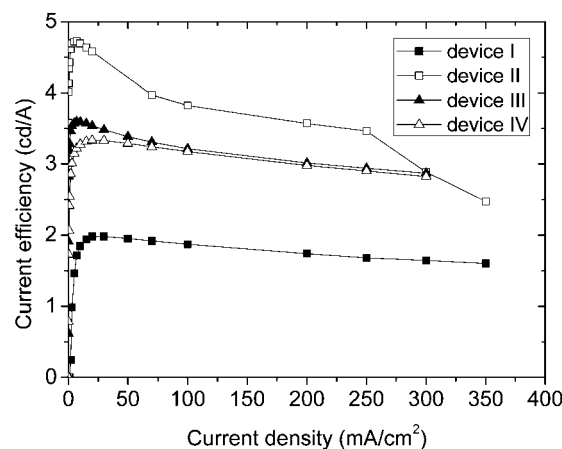
Table 3 Electroluminescence performance for B3 and B4

Device	V_{on} (V) ^a	L_{max} (Voltage) (cd m ⁻²) (V) ^b	η_{p} (lm W ⁻¹) ^{c/d}	η_{c} (cd A ⁻¹) ^{e/f}	η_{ext} (%) ^{g/h}	L (cd m ⁻²) ⁱ	V (V) ^j	λ_{em} (FWHM) (nm) ^k	CIE (x,y) ^l	
B3	I	2.6	7429(7.4)	2.47/2.68	2.72/2.72	1.90/1.91	543.1	3.5	468(60)	(0.14,0.19)
	II	2.8	12250(8.6)	3.17/3.50	4.29/4.29	2.64/2.66	857.8	4.2	468(64)	(0.15,0.23)
	III	2.7	10750 (8.8)	2.60/2.83	3.63/3.63	2.41/2.42	725.0	4.4	468(60)	(0.14,0.21)
B4	I	2.5	5610(8.0)	1.76/1.79	1.98/1.98	1.92/1.93	396.3	3.5	452(60)	(0.15,0.12)
	II	2.7	8656(7.6)	3.52/4.52	4.58/4.72	3.87/3.94	915.8	4.1	456(60)	(0.15,0.14)
	III	2.6	8612(7.5)	2.88/3.50	3.54/3.60	3.54/3.60	707.5	3.9	456(60)	(0.15,0.14)
	IV	2.6	8472(8.7)	2.64/2.83	3.33/3.33	2.64/2.66	666.6	4.3	456(60)	(0.16,0.16)

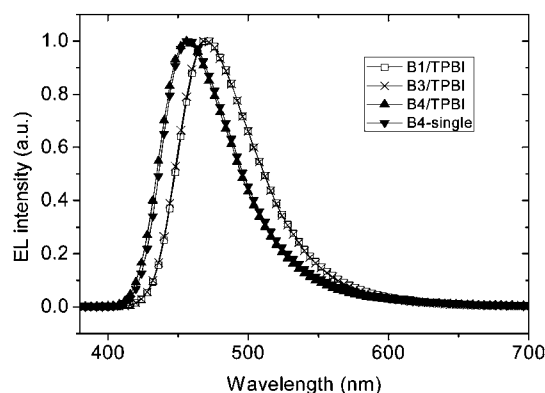
^a V_{on} : turn-on voltage. ^b L_{max} : maximum luminance. Voltage: voltage at the maximum luminance. ^c η_{p} : power efficiency measured at 20 mA cm⁻². ^d Maximum power efficiency. ^e η_{c} : current efficiency measured at 20 mA cm⁻². ^f Maximum current efficiency. ^g η_{ext} : external quantum efficiency measured at 20 mA cm⁻². ^h Maximum external quantum efficiency. ⁱ L : luminance measured at 20 mA cm⁻². ^j V : voltage at 20 mA cm⁻². ^k λ_{em} : emission wavelength at 20 mA cm⁻². FWHM: full width at half maximum at 20 mA cm⁻². ^l Values at 20 mA cm⁻².

B4 are 3.70, 3.63, and 3.54 cd A⁻¹, respectively, all of which are higher than that of B1 (2.34 cd A⁻¹). The shortest phenyl rings bridge might promote the bipolar quench to affect the device performance, agreeing with data of the quantum yield in the toluene. Generally, the performance of the device II for all the compounds is better than those of the device I. This was attributed to the closer HOMO energy level between B1–4 and NPB, the small energy barrier between the B1–4 and anode would facilitate the hole injection. In contrast, the larger energy level between bipolar compounds and the cathode will increase the difficulty of electron injection from the cathode to the anthracene derivatives. In device II, an electron-transporting layer (TPBI) was inserted between the B1–4 and cathode, therefore, the energy barrier between the cathode and B1–4 will be effectively reduced, which will increase the electron injection and improve the device performance. Although another hole-transporting layer (NPB) was added in the device III, device II exhibited better performance than that of device III, this maybe due to the interface effect between layers. The result also displays that the blue emitters contain the excellent hole-transporting and electron-transporting properties, which is one important condition of the simplification of OLEDs.

For compounds B1, B3, and B4, all three types of devices emit the light in blue region with a narrow FWHM (full width at half maximum), and the EL spectra are almost identical with PL spectra in the film. Fig. 5 illustrated the EL spectra of the device II for the compounds B1, B3 and B4 at 20 mA cm⁻². The spectra

**Fig. 3** Current density–voltage–luminance (I – V – L) characteristics of devices I–IV for B4.**Fig. 4** The current density-current efficiency characteristics of device I–IV for B4.

of B1 and B3 showed a little red-shift compared to that of B4, because the shorter phenyl bridge could increase the coplanarity between the electron-donating triphenylamine and the light-emitting anthracene core. It is interesting that an orange emission peak at around 550 nm was observed in the EL spectra of B2 (see in Fig. S4†). For three devices, at a low current density (<5 mA cm⁻²), the orange emission peak was too strong to make the devices emit near white light. As increasing the current density, the orange peak decreases to reach a steady value about

**Fig. 5** EL spectra of the device II for the compounds B1, B3 and B4 at 20 mA cm⁻².

a half of the blue peak in intensity. This phenomenon should be ascribed to the electromer formation of B2, since there is no evidence of excimer formation from the film and solution PL spectrum.

Importantly, a single-layer device based on B4 with the structure of ITO/B4 (80 nm)/LiF (1 nm)/Al (100 nm) was also fabricated to exhibit its excellent bipolar characteristic and light-emitting properties. The EL performance and spectra were also displayed in the Table 3 and Fig. 3, 4, and 5, which were comparable with those of the multilayer devices. These good results show that B4 can be used as the promising blue light-emitting material in the single layer OLEDs. As a result, we achieved a current efficiency of 3.33 cd A^{-1} with a $\text{CIE}_{(x,y)}$ of (0.16, 0.16) at 20 mA cm^{-2} and a maximum brightness of 8472 cd m^{-2} at 8.7 V, which is better than the previous reports about the single-layer devices.^{8–20}

Conclusions

In summary, we have synthesized a series of bipolar anthracene derivatives containing hole-transporting triphenylamine and electron-transporting benzimidazole moieties. They possess good thermal properties with the T_g higher than $140 \text{ }^\circ\text{C}$. The PL spectra were largely affected by the polarity of the solvent and the phenyl bridge length. A series of devices based on these derivatives exhibit their excellent bipolar properties and low operating voltage. Due to the electromer formation of B2, we can get the white emission OLEDs with a single component at a low current density ($< 5 \text{ mA cm}^{-2}$), while others devices emit blue light with a narrow FWHM about 60 nm. Moreover, an un-optimized single layer device for B4 exhibited a current efficiency of 3.33 cd A^{-1} with a pure blue color of $\text{CIE}_{(x,y)}$ of (0.16, 0.16) at 20 mA cm^{-2} and a maximum brightness of 8472 cd m^{-2} at 8.7 V. This EL performance is the best among reports for the pure blue single-layer OLEDs in the previous literatures.

Experimental

General information

Unless otherwise specified, all reactions and manipulations were performed under nitrogen atmosphere using standard Schlenk techniques. All chemical reagents were used as received from commercial sources without further purification. And the solvents were dried using standard procedures. ^1H and ^{13}C NMR spectra were recorded on Brüker AV-400, spectrometer tetramethylsilane (TMS) as the internal standard. High resolution mass spectrometric measurements were carried out using a Brüker autoflex MALDI-TOF mass spectrometer. UV-vis spectra were obtained on a Varian Cary 200 spectrophotometer. Fluorescence spectra were obtained on a Perkin Elmer LS55 luminescence spectrometer with the excitation at 380 nm. To measure the fluorescence quantum yields (Φ_f), degassed solutions of the compounds in toluene were prepared. The concentration was adjusted so that the absorbance of the solution would be lower than 0.1. The excitation was performed at 380 nm, and 9,10-diphenylanthracene (DPA) in the solution of cyclohexane, which has $\Phi_f = 0.9$, was used as a standard. The differential scanning calorimetry (DSC) analysis was performed under a nitrogen atmosphere on a TA Instruments DSC 2920 with

a heating and cooling scan rate of $20 \text{ }^\circ\text{C}/\text{min}$. Thermogravimetric analysis was undertaken using a TGA instrument under a nitrogen atmosphere with a heating scan rate of $20 \text{ }^\circ\text{C}/\text{min}$. Cyclic voltammetric (CV) measurements were carried out in a conventional three electrode cell using a Pt button working electrode of 2 mm in diameter, a platinum wire counter electrode, and a SCE reference electrode on a computer-controlled EG&G Potentiostat/Galvanostat model 283 at room temperature. Reduction CV of all compounds was performed in dichloromethane containing Bu_4NPF_6 (0.1 M) as the supporting electrolyte. The $E_{1/2}$ values were determined by $(E_{\text{pa}} + E_{\text{pc}})/2$, where E_{pa} and E_{pc} are the anodic and cathodic peak potentials, respectively. Ferrocene was used as an external standard. Electrochemistry was done at a scan rate of 100 mV/s . Density functional theory (DFT) was calculated at the B3LYP/6-31G* level.

Synthesis

Triphenylamine boronic acid (BA1), 4-(diphenylamino)-biphenyl-4'-boronic acid (BA2),²⁹ 4-(1-phenyl-1*H*-benzimidazol-2-yl)-phenylboronic acid (BA3)^{20d} and 1-phenyl-1*H*-2-(4-bromophenyl)-benzimidazole (BA4)^{20d} were prepared according to the literatures. The bipolar compounds B1–B4 were synthesized following the similar procedures with Suzuki aryl-aryl coupling reactions.

Synthesis of 9-anthracene boronic acid (1). Under the atmosphere of nitrogen, 9-bromoanthracene (2.57 g, 10 mmol) was added to 30 ml of dry THF solution and stirred for 30 min at $-78 \text{ }^\circ\text{C}$, then *n*-BuLi (8 ml, 15 mmol, 1.6 M solution in hexane) was added. The mixture was stirred for 2 h. Triisopropylborate (2.9 g, 8.6 mmol) was added to the reaction mixture. After the addition was completed, the solution was warmed slowly to room temperature and stirred overnight. The reaction mixture was added to an aqueous solution of HCl (2 N) and extracted with dichloromethane. The organic extracts were washed with brine and H_2O , and dried with anhydrous MgSO_4 and filtered. After the solvent was evaporated, the crude product was crystallized from dichloromethane and *n*-hexane to afford 1.47 g of white solid (66.2%). ^1H NMR: (400 MHz, DMSO, δ): 8.81 (s, 2 H), 8.52 (s, 1 H), 8.05–8.08 (m, 2 H), 7.97–8.00 (m, 2 H), 7.47–7.52 (4 H).

Synthesis of 9-(4-bromophenyl)-anthracene (2). 9-anthracene boronic acid (1) (0.11 g, 0.5 mmol) and 4-bromo-iodobenzene (0.154 g, 0.55 mmol) were mixed in 10 ml of THF. K_2CO_3 (2.0 M, 10 ml) was added, and the mixture was stirred with magnetic stirring. Then tetrakis (triphenylphosphine) palladium (10 mg, 0.0075 mmol) was added to the mixture. The reaction solution was heated under reflux for 12 h under the atmosphere of nitrogen. After the mixture cooled, the solvent was evaporated and the product was extracted with dichloromethane. The organic was washed with brine and water, and then dried by anhydrous MgSO_4 . The solvent was evaporated, and the residue was purified by using column chromatography with DCM : *n*-Hexane = 1 : 6 eluent to afford a white solid (0.14 g, 84.3%). ^1H NMR: (400 MHz, CDCl_3 , δ): 8.51 (s, 1 H), 8.04–8.06 (d, $J = 8.4 \text{ Hz}$, 2 H), 7.71–7.73 (d, $J = 6.4 \text{ Hz}$, 2 H), 7.61–7.64 (d, $J = 8.8 \text{ Hz}$, 2 H), 7.45–7.49 (m, 2 H), 7.35–7.39

(m, 2 H), 7.30–7.24 (m, 2 H). ^{13}C NMR (400 MHz, CDCl_3 , δ): 137.69, 135.42, 132.95, 131.61, 131.26, 130.02, 128.41, 126.96, 126.41, 125.61, 125.17, 121.70. MALDI-TOF-MS (m/z): [M^+] calcd for $\text{C}_{20}\text{H}_{13}\text{Br}$, 334.0187; found, 334.0170.

Synthesis of 9-[4-(1-phenyl-1*H*-benzimidazol-2-yl)-phenyl]-anthracene (3). 1-phenyl-1*H*-2-(4-bromophenyl)-benzimidazole (BA4) (1.0 g, 2.87 mmol) and 9-anthracene boronic acid (**1**) (0.64 g, 2.87 mmol) were mixed in 10 ml of THF. K_2CO_3 (2.0 M, 10 ml) was added, and the mixture was stirred with magnetic stirring. Then tetrakis (triphenylphosphine) palladium (10 mg, 0.0075 mmol) was added to the mixture. The reaction solution was heated under reflux for 12 h under the atmosphere of nitrogen. After the mixture cooled, the solvent was evaporated and the product was extracted with dichloromethane. The organic was washed with brine and water, and then dried by anhydrous MgSO_4 . The solvent was evaporated, and the residue was purified by using column chromatography with ethanyl acetic : n-hexane = 1 : 3 eluent to afford a yellow solid (1.15 g, 89.8%). ^1H NMR: (400 MHz, CDCl_3 , δ): 8.49 (s, 1 H), 8.03–8.05 (d, $J = 8.4$ Hz, 2 H), 7.94–7.96 (d, $J = 8.0$ Hz, 1 H), 7.78–7.80 (d, $J = 8.4$ Hz, 2 H), 7.57–7.63 (m, 4 H), 7.44–7.54 (m, 5 H), 7.31–7.40 (m, 7 H). ^{13}C NMR (400 MHz, CDCl_3 , δ): 152.23, 143.02, 140.12, 137.31, 136.99, 135.94, 131.25, 129.97, 129.93, 129.35, 129.17, 128.77, 128.38, 127.50, 126.88, 126.49, 125.51, 125.13, 123.45, 123.10, 119.88, 110.54. MALDI-TOF-MS (m/z): [M^+] calcd for $\text{C}_{33}\text{H}_{22}\text{N}_2$, 446.1788; found: 446.1808.

Synthesis of 9-bromo-10-[4-(1-phenyl-1*H*-benzimidazol-2-yl)-phenyl]-anthracene (4). 9-[4-(1-phenyl-1*H*-benzimidazol-2-yl)-phenyl]-anthracene (**3**) (0.78 g, 1.76 mmol), *N*-bromosuccinimide (NBS) (0.313 g, 1.76 mmol) was mixed with 10 ml of chloroform. The reaction mixture was heated to 50 °C for 2 h under nitrogen. After the reaction finished, the solvent was evaporated. The residue was crystallized from acetone and methanol to afford a yellow solid (0.80 g, 87.3%). ^1H NMR: (400 MHz, CDCl_3 , δ): 8.60–8.62 (d, $J = 8.4$ Hz, 2 H), 7.94–7.96 (d, $J = 8.0$ Hz, 1 H), 7.79–7.81 (d, $J = 8.0$ Hz, 2 H), 7.54–7.62 (m, 7 H), 7.47–7.48 (d, $J = 8.4$ Hz, 2 H), 7.33–7.41 (m, 5 H), 7.32 (m, 2 H). ^{13}C NMR (400 MHz, CDCl_3 , δ): 152.07, 143.06, 139.70, 137.37, 136.99, 136.73, 131.26, 130.75, 130.16, 130.03, 129.56, 129.42, 128.85, 127.93, 127.52, 127.10, 127.01, 125.76, 123.55, 123.17, 123.11, 119.95, 110.59. MALDI-TOF-MS (m/z): [$M + \text{H}$] $^+$ calcd for $\text{C}_{33}\text{H}_{22}\text{BrN}_2$, 527.0956; found: 527.0978.

Synthesis of 9-[4-(1-phenyl-1*H*-benzimidazol-2-yl)-biphenyl-4'-yl]-anthracene (5). 9-(4-bromophenyl)-anthracene (**2**) (0.50 g, 1.5 mmol), 4-(1-phenyl-1*H*-benzimidazol-2-yl)-benzene boronic acid (BA3) (0.47 g, 1.5 mmol) were mixed in 10 ml of THF. K_2CO_3 (2.0 M, 10 ml) was added, and the mixture was stirred with magnetic stirring. Then tetrakis (triphenylphosphine) palladium (10 mg, 0.0075 mmol) was added to the mixture. The reaction solution was heated under reflux for 12 h under the atmosphere of nitrogen. After the mixture cooled, the solvent was evaporated and the product was extracted with dichloromethane. The organic product was washed with brine and water, and then dried by anhydrous MgSO_4 . The solvent was evaporated, and the residue was purified by using column chromatography with ethanyl acetic : n-hexane = 1 : 3 eluent to afford

a yellow solid (0.783 g, 71.5%). ^1H NMR: (400 MHz, CDCl_3 , δ): 8.50 (s, 1 H), 8.03–8.05 (d, $J = 8.4$ Hz, 2 H), 7.92–7.94 (d, $J = 8.0$ Hz, 1 H), 7.79–7.81 (d, $J = 8.0$ Hz, 2 H), 7.69–7.71 (m, 6 H), 7.43–7.56 (m, 7 H), 7.33–7.40 (m, 5 H), 7.28–7.29 (m, 2 H). ^{13}C NMR (400 MHz, CDCl_3 , δ): 152.10, 143.08, 141.59, 139.08, 138.33, 137.31, 137.05, 136.40, 131.78, 131.33, 130.15, 129.95, 128.93, 128.63, 128.37, 127.48, 126.94, 126.69, 125.42, 125.12, 123.39, 123.05, 119.84, 110.46. MALDI-TOF-MS (m/z): [M^+] calcd for $\text{C}_{39}\text{H}_{26}\text{N}_2$, 522.2101; found, 522.2123.

Synthesis of 9-bromo-10-[4-(1-phenyl-1*H*-benzimidazol-2-yl)-biphenyl-4'-yl]-anthracene (6). 9-[4-(1-phenyl-1*H*-benzimidazol-2-yl)-biphenyl-4'-yl]-anthracene (**5**) (0.52 g, 1 mmol), *N*-bromosuccinimide (NBS) (0.187 g, 1.05 mmol) was mixed in 10 ml of chloroform. The reaction mixture was heated to 50 °C for 2 h under nitrogen. After the reaction finished, the solvent was evaporated. The residue was crystallized from acetone and methanol to afford a yellow solid (0.54 g, 90.0%). ^1H NMR: (400 MHz, CDCl_3 , δ): 8.61–8.63 (d, $J = 8.8$ Hz, 2 H), 7.92–7.94 (d, $J = 8.0$ Hz, 1 H), 7.80–7.82 (d, $J = 8.0$ Hz, 2 H), 7.69–7.72 (m, 5 H), 7.46–7.62 (m, 8 H), 7.35–7.41 (m, 5 H), 7.29–7.30 (m, 2 H). ^{13}C NMR (400 MHz, CDCl_3 , δ): 152.04, 142.99, 141.47, 139.41, 137.91, 137.29, 137.20, 137.02, 131.68, 130.97, 130.20, 129.99, 129.00, 128.68, 127.89, 127.49, 127.27, 127.03, 126.98, 126.93, 125.65, 123.45, 123.11, 122.89, 119.83, 110.49. MALDI-TOF-MS (m/z): [$M + \text{H}$] $^+$ calcd for $\text{C}_{39}\text{H}_{26}\text{BrN}_2$, 603.1271; found, 603.1277.

Synthesis of 9-[4-(1-phenyl-1*H*-benzimidazol-2-yl)-phenyl]-10-[4-(diphenlamino)-phenyl]-anthracene (B1). 9-bromo-10-[4-(1-phenyl-1*H*-benzimidazol-2-yl)-phenyl]-anthracene (**4**) (0.315 g, 0.6 mmol), 4-(diphenylamino)-phenyl boronic acid (0.173 g, 0.6 mmol) 10 ml of THF. K_2CO_3 (2.0 M, 10 ml) was added, and the mixture was stirred with magnetic stirring. Then tetrakis (triphenylphosphine) palladium (10 mg, 0.0075 mmol) was added to the mixture. The reaction solution was heated under reflux for 12 h under N_2 . After the mixture cooled, the solvent was evaporated and the product was extracted with dichloromethane. The organic was washed with brine and water, and then dried by anhydrous MgSO_4 . The solvent was evaporated, and the residue was purified by using column chromatography with ethanyl acetic : n-hexane = 1 : 3 eluent to afford a yellow solid (0.353 g, 85.3%). ^1H NMR: (400 MHz, CDCl_3 , δ): 7.94–7.96 (d, $J = 8.0$ Hz, 1 H), 7.81–7.85 (m, 4 H), 7.58–7.66 (m, 4 H), 7.48–7.55 (m, 3 H), 7.25–7.44 (m, 21 H), 7.06–7.10 (m, 2 H). ^{13}C NMR (400 MHz, CDCl_3 , δ): 152.27, 147.76, 147.17, 143.09, 140.50, 137.35, 137.05, 135.88, 132.41, 132.05, 131.45, 130.02, 129.98, 129.70, 129.38, 129.23, 128.77, 127.53, 127.13, 126.67, 125.19, 124.99, 124.69, 123.45, 123.09, 123.03, 119.92, 110.54. MALDI-TOF-MS (m/z): [M^+] calcd for $\text{C}_{51}\text{H}_{35}\text{N}_3$, 689.2825; found, 689.2862.

Synthesis of 9-[4-(diphenlamino)-biphenyl-4'-yl]-10-[4-(1-phenyl-1*H*-benzimidazol-2-yl)-phenyl]-anthracene (B2). Yellow solid (74.6%). ^1H NMR: (400 MHz, CDCl_3 , δ): 7.95–7.97 (d, $J = 8.0$ Hz, 2 H), 7.77–7.84 (m, 6 H), 7.59–7.68 (m, 6 H), 7.49–7.54 (m, 5 H), 7.44–7.46 (d, $J = 8.0$ Hz, 2 H), 7.28–7.36 (m, 11 H), 7.17–7.23 (m, 6 H), 7.04–7.06 (m, 2 H). ^{13}C NMR (400 MHz, CDCl_3 , δ): 152.27, 147.67, 147.37, 143.10, 140.46, 139.75, 137.36, 137.21, 137.06, 136.07, 134.61, 131.72, 131.46, 130.00, 129.88,

129.67, 129.42, 129.32, 128.79, 127.78, 127.54, 127.07, 126.69, 126.57, 125.22, 125.08, 124.50, 123.92, 123.46, 123.10, 123.00, 119.93, 110.55. MALDI-TOF-MS (m/z): [M^+] calcd for $C_{57}H_{39}N_2$, 765.3138; found, 765.3196.

Synthesis of 9-[4-(1-phenyl-1H-benzimidazol-2-yl)-biphenyl-4'-yl]-10-[4-(diphenylamino)-phenyl]-anthracene (B3). Yellow solid (71.5%). 1H NMR: (400 MHz, $CDCl_3$, δ): 7.92–7.94 (d, $J = 8.0$ Hz, 2 H), 7.83–7.87 (m, 4 H), 7.73–7.75 (m, 6 H), 7.52–7.58 (m, 5 H), 7.25–7.42 (m, 21 H), 7.07–7.10 (m, 2 H). ^{13}C NMR (400 MHz, $CDCl_3$, δ): 152.13, 147.78, 147.16, 143.08, 141.63, 139.10, 138.70, 137.32, 137.17, 137.08, 136.34, 132.52, 132.09, 131.89, 130.07, 129.97, 129.91, 129.39, 128.94, 128.65, 127.51, 127.13, 127.01, 126.92, 126.87, 125.12, 125.00, 124.69, 123.40, 123.09, 123.07, 119.85, 110.47. MALDI-TOF-MS (m/z): [M^+] calcd for $C_{57}H_{39}N_2$, 765.3138; found, 765.3109.

Synthesis of 9-[4-(1-phenyl-1H-benzimidazol-2-yl)-biphenyl-4'-yl]-10-[4-(diphenylamino)-biphenyl-4'-yl]-anthracene (B4). Yellow solid (71.7%). MALDI-TOF-MS (m/z): [$M + H$] $^+$ calcd for $C_{63}H_{44}N_3$, 842.3529; found, 842.3582.

Device fabrication

Prior to the deposition of organic materials, indium-tin-oxide (ITO)/glass was cleaned with a routine cleaning procedure and pretreated with oxygen plasma, and then coated with a polymerized fluorocarbon (CF_x) film. Devices were fabricated under about 10^{-6} Torr base vacuum in a thin-film evaporation coater. The current–voltage–luminance characteristics were measured with a diode array rapid scan system using a Photo Research PR650 spectrophotometer and a computer-controlled, programmable, direct-current (DC) source. All measurements were carried out in ambient atmosphere at room temperature.

Acknowledgements

This work was financially supported by NSFC/China, National Basic Research 973 Program and Hong Kong Baptist University.

References

- (a) C. W. Tang and S. A. Van Slyke, *Appl. Phys. Lett.*, 1987, **51**, 913; (b) L. S. Huang and C. H. Chen, *Mater. Sci. Eng., R*, 2002, **39**, 143.
- F. C. Chen, T. Yang, M. E. Thompson and J. Kido, *Appl. Phys. Lett.*, 2002, **80**, 2308.
- B. W. D'Andrade and S. R. Forrest, *Adv. Mater.*, 2004, **16**, 1585.
- H. Doi, M. Kinoshita, K. Okumoto and Y. Shiota, *Chem. Mater.*, 2003, **15**, 1080.
- (a) D. Y. Kondakov, *J. Appl. Phys.*, 2006, **99**, 024901; (b) R. Meerheim, S. Scholz, S. Olthof, G. Schwartz, S. Reineke, K. Walzer and K. Leo, *J. Appl. Phys.*, 2008, **104**, 014510; (c) H. H. Fong, W. C. H. Choy, K. N. Hui and Y. J. Liang, *Appl. Phys. Lett.*, 2006, **88**, 113510.
- (a) Q. S. Mohammad and S. S. Manoharan, *J. Appl. Phys.*, 2005, **97**, 096101; (b) S.-J. Su, Y. Takahashi, T. Chiba, T. Takeda and J. Kido, *Adv. Funct. Mater.*, 2009, **19**, 1260; (c) N. Li, P. Wang, S.-L. Lai, W. Liu, C.-S. Lee, S.-T. Lee and Z. Liu, *Adv. Mater.*, 2010, **22**, 527; (d) T. Earmme, E. Ahmed and S. A. Jenekhe, *J. Phys. Chem. C*, 2009, **113**, 18448; (e) S. Tao, S. L. Lai, J. Yu, Y. Jiang, Y. Zhou, C.-S. Lee, X. Zhang and S.-T. Lee, *J. Phys. Chem. C*, 2009, **113**, 16792.
- K. R. Justin Thomas, J. T. Lin, Y.-T. Tao and C.-H. Chuen, *Chem. Mater.*, 2004, **16**, 5437.

- (a) K. R. Justin Thomas, M. Velusamy, J. T. Lin, Y.-T. Tao and C.-H. Chuen, *Adv. Funct. Mater.*, 2004, **14**, 387; (b) K. R. Justin Thomas, J. T. Lin, Y.-T. Tao and C. H. Chuen, *J. Mater. Chem.*, 2002, **12**, 3516.
- C.-T. Chen, J.-S. Lin, M. V. R. K. Moturu, Y.-W. Lin, W. Yi, Y.-T. Tao and C.-H. Chien, *Chem. Commun.*, 2005, 3980.
- L.-H. Chan, H.-C. Yeh and C.-T. Chen, *Adv. Mater.*, 2001, **13**, 1637.
- H.-C. Yeh, R.-H. Lee, L.-H. Chan, T.-Y. J. Lin, C.-T. Chen, E. Balasubramaniam and Y.-T. Tao, *Chem. Mater.*, 2001, **13**, 2788.
- (a) F.-M. Hsu, C.-H. Chien, C.-F. Shu, C.-H. Lai, C.-C. Hsieh, K.-W. Wang and P.-T. Chou, *Adv. Funct. Mater.*, 2009, **19**, 2834; (b) J. M. Hancock, A. P. Gifford, Y. Zhu, Y. Lou and S. A. Jenekhe, *Chem. Mater.*, 2006, **18**, 4924; (c) Y. Zhu, A. P. Kulkarni, P.-T. Wu and S. A. Jenekhe, *Chem. Mater.*, 2008, **20**, 4200; (d) F.-M. Hsu, C.-H. Chien, P.-I. Shih and C.-F. Shu, *Chem. Mater.*, 2009, **21**, 1017.
- S. Tao, L. Li, J. Yu, Y. Jiang, Y. Zhou, C.-S. Lee, S.-T. Lee, X. Zhang and O. Kwon, *Chem. Mater.*, 2009, **21**, 1284.
- S. Takizawa, V. A. Montes and J. P. Anzenbacher, *Chem. Mater.*, 2009, **21**, 2452.
- (a) Z. Q. Gao, M. Luo, X. H. Sun, H. L. Tam, M. S. Wong, B. X. Mi, P. F. Xia, K. W. Cheah and C. H. Chen, *Adv. Mater.*, 2009, **21**, 688; (b) T. H. Lee, K. L. Tong, S. K. So and L. M. Leung, *Synth. Met.*, 2005, **155**, 116; (c) Z. Ge, T. Hayakawa, S. Ando, M. Ueda, T. Akiike, H. Miyamoto, T. Kajita and M. Kakimoto, *Org. Lett.*, 2008, **10**, 421; (d) Y. Sun, L. Duan, P. Wei, J. Qiao, G. Dong, L. Wang and Y. Qiu, *Org. Lett.*, 2009, **11**, 2069; (e) T.-H. Huang, J. T. Lin, L.-Y. Chen, Y.-T. Lin and C.-C. Wu, *Adv. Mater.*, 2006, **18**, 602.
- S.-L. Lin, L.-H. Chan, R.-H. Lee, M.-Y. Yen, C.-T. Kuo and R.-J. Jeng, *Adv. Mater.*, 2008, **20**, 3947.
- K. R. J. Thomas, M. Velusamy, J. T. Lin, C.-H. Chuen and Y.-T. Tao, *Chem. Mater.*, 2005, **17**, 1860.
- (a) H.-H. Chou and C.-H. Cheng, *Adv. Mater.*, 2010, **22**, 2468; (b) Y. Tao, Q. Wang, C. Yang, Z. Zhang, T. Zou, J. Qin and D. Ma, *Angew. Chem., Int. Ed.*, 2008, **47**, 8104.
- (a) C.-J. Kuo, T.-Y. Li, C.-C. Lien, C.-H. Liu, F.-I. Wu and M.-J. Huang, *J. Mater. Chem.*, 2009, **19**, 1865; (b) Z. H. Li, M. S. Wong, H. Fukutani and Y. Tao, *Org. Lett.*, 2006, **8**, 4271.
- (a) Y.-L. Liao, C.-Y. Lin, K.-T. Wong, T.-H. Hou and W.-Y. Huang, *Org. Lett.*, 2007, **9**, 4511; (b) M.-Y. Lai, C.-H. Chen, W.-S. Huang, J. T. Lin, T.-H. Ke, L.-Y. Chen, M.-H. Tsai and C.-C. Wu, *Angew. Chem., Int. Ed.*, 2008, **47**, 581; (c) C.-H. Chen, W.-S. Huang, M.-Y. Lai, W.-C. Tsao, J. T. Lin, Y.-H. Wu, T.-H. Ke, L.-Y. Chen and C.-C. Wu, *Adv. Funct. Mater.*, 2009, **19**, 2661; (d) Z. Ge, T. Hayakawa, S. Ando, M. Ueda, T. Akiike, H. Miyamoto, T. Kajita and M. Kakimoto, *Adv. Funct. Mater.*, 2008, **18**, 584.
- K. Danel, T.-H. Huang, J. T. Lin, Y.-T. Tao and C. H. Chuen, *Chem. Mater.*, 2002, **14**, 3860.
- (a) M.-H. Ho, Y.-S. Wu, S.-W. Wen, M.-T. Lee, T.-M. Chen and C. H. Chen, *Appl. Phys. Lett.*, 2006, **89**, 252903; (b) C. W. Tang, S. A. Van Slyke and C. H. Chen, *J. Appl. Phys.*, 1989, **65**, 3610.
- (a) Y. Kan, L. Wang, L. Duan, Y. Hu, G. Wu and Y. Qiu, *Appl. Phys. Lett.*, 2004, **84**, 1513; (b) Y.-H. Kim, H.-C. Jeong, S.-H. Kim, K. Yang and S.-K. Kwon, *Adv. Funct. Mater.*, 2005, **15**, 1799; (c) Y.-Y. Lyu, J. Kwak, O. Kwon, S.-H. Lee, D. Kim, C. Lee and K. Char, *Adv. Mater.*, 2008, **20**, 2720; (d) S.-K. Kim, B. Yang, Y. Ma, J.-H. Lee and J.-W. Park, *J. Mater. Chem.*, 2008, **18**, 3376; (e) C.-H. Wu, C.-H. Chien, F. M. Hsu, P.-I. Shih and C.-F. Shu, *J. Mater. Chem.*, 2009, **19**, 1464; (f) M.-X. Yu, J.-P. Duan, C.-H. Lin, C.-H. Cheng and Y.-T. Tao, *Chem. Mater.*, 2002, **14**, 3958; (g) J. Huang, B. Xu, J.-H. Su, C. H. Chen and H. Tian, *Tetrahedron*, 2010, **66**, 7577.
- M.-H. Ho, T. M.-Hsieh, K.-H. Lin, T.-M. Chen, J.-F. Chen and C. H. Chen, *Appl. Phys. Lett.*, 2006, **94**, 023306.
- K. Okumoto, H. Kanno, Y. Hamaa, H. Takahashi and K. Shibata, *Appl. Phys. Lett.*, 2006, **89**, 063504.
- (a) L. Wang, M.-F. Lin, W.-K. Wong, K.-W. Cheah, H.-L. Tam, Z.-Q. Gao and C. H. Chen, *Appl. Phys. Lett.*, 2007, **91**, 183504; (b) L. Wang, W.-Y. Wong, M.-F. Lin, W.-K. Wong, K.-W. Cheah, H.-L. Tam and C. H. Chen, *J. Mater. Chem.*, 2008, **18**, 4529.
- T. M. Adms and S. Ramdas, *Acta Crystallogr., Sect. B: Struct. Crystallogr. Cryst. Chem.*, 1979, **35**, 679.
- (a) P. Wang, Z. Xie, Z. Hong, J. Tang, O. Wong, C.-S. Lee, N. Wong and S. Lee, *J. Mater. Chem.*, 2003, **13**, 1894; (b) K. R. J. Thomas, J. T. Lin, Y.-T. Tao and C.-H. Chuen, *Chem. Mater.*, 2002, **14**, 3852.
- Z. H. Li, M. S. Wong, Y. Tao and M. D'Iorio, *J. Org. Chem.*, 2004, **69**, 921.